Research Article | Vol. 26, No. 21 | 15 Oct 2018 | OPTICS EXPRESS 27705
Optics EXPRESS

Loss-tolerant quantum dense metrology with SU(1,1) interferometer

YUHONG LIU,[1] JIAMIN LI,[1] LIANG CUI,[1] NAN HUO,[1] SYED M. ASSAD,[2] XIAOYING LI,[1,*] AND Z. Y. OU[1,3,4]

[1] *College of Precision Instrument and Opto-Electronics Engineering, Key Laboratory of Opto-Electronics Information Technology, Ministry of Education, Tianjin University, Tianjin 300072, China*
[2] *Department of Quantum Science, The Australian National University, Canberra ACT 0200, Australia*
[3] *Department of Physics, Indiana University-Purdue University Indianapolis, Indianapolis, IN 46202, USA*
[4] *zheyuou@tju.edu.cn*
[*] *xiaoyingli@tju.edu.cn*

Abstract: Heisenberg uncertainty relation in quantum mechanics sets the limit on the measurement precision of non-commuting observables in one system, which prevents us from measuring them accurately at the same time. However, quantum entanglement between two systems allows us to infer through Einstein-Podolsky-Rosen correlations two conjugate observables with precision better than what is allowed by Heisenberg uncertainty relation. With the help of the newly developed SU(1,1) interferometer, we implement a scheme to jointly measure information encoded in multiple non-commuting observables of an optical field with a signal-to-noise ratio improvement of about 20% over the classical limit on all measured quantities simultaneously. This scheme can be generalized to the joint measurement of information in arbitrary number of non-commuting observables.

1. Introduction

Quantum properties of light were applied to precision phase measurement as early as in 1980s, beating the shot noise limit (SNL) set by the quantum physics for the classical systems using classical techniques [1–3]. The basic idea is to reduce the quantum noise in the measurement with some novel quantum states of light. Recently, the topic of multi-parameter estimation and measurement has also attracted much attention because it is related to the fundamental quantum measurement process as well as practical applications in quantum imaging and sensing [4–8]. However, because of the Heisenberg uncertainty relation (HUR) on two non-commuting observables, quantum noise reduction in one observable inevitably leads to the noise increase in the other. Thus, it seems impossible to beat the SNL simultaneously in joint measurement of non-commuting observables.

On the other hand, quantum correlation via quantum entanglement provides us with a remedy to circumvent the aforementioned dilemma. Braunstein and Kimble proposed in 2000 a quantum dense coding scheme in which one of two optical fields with Einstein-Podolsky-Rosen (EPR) type of quantum entanglement is used to probe both phase and amplitude modulations simultaneously [9]. With the help of quantum entanglement, it is possible to jointly measure the phase and amplitude modulations with measurement precision simultaneously beating the classical limit set by the vacuum noise. A variation of the scheme was proposed by Zhang and Peng [10] and experimentally implemented by Li et al. [11]. More recently, it was applied to a prototype interferometer for improved performance in gravitational wave detection in the form of quantum dense metrology [12].

However, the aforementioned quantum dense metrology scheme requires the superposition of the two entangled fields by a beam splitter for the quantum noise cancellation to increase measurement sensitivity. This means that the two entangled fields must be frequency degenerate,

#332922 https://doi.org/10.1364/OE.26.027705
Journal © 2018 Received 6 Jun 2018; revised 11 Aug 2018; accepted 13 Aug 2018; published 9 Oct 2018

Optics EXPRESS

which excludes many possible entangled sources for this application. Furthermore, the scheme is extremely sensitive to passive losses such as those occurred during propagation and detection because quantum noise reduction technique is notoriously prone to losses.

In this paper, we implement a new quantum dense metrology scheme with an SU(1,1) interferometer that was recently developed for quantum metrology in phase measurement [13–21]. We are able to make use of frequency non-degenerate entanglement to perform joint measurement of phase and amplitude modulations or any other modulations at arbitrary quadrature angles on one optical fields with measurement precision beating the classical limit simultaneously while avoiding the aforementioned difficulties. Furthermore, using the unique loss-tolerant property of SU(1,1) interferometer, we are able to make joint measurement on multiple (more than 2) modulations at different quadrature angles.

2. Theory

While the Heisenberg uncertainty relation (HUR) is on two non-commuting observables of one *single* system, quantum mechanics allows perfect correlations between non-commuting observables of *two* systems. Einstein, Podolsky, and Rosen showed in a seminal paper [22] that there exists such a quantum state of a two-particle system that exhibits perfect correlations not only between the positions of the two particles but also between their momenta. This is so because the difference of their position operators $\hat{x}_1 - \hat{x}_2$ and the sum of their momenta operators $\hat{p}_1 + \hat{p}_2$ commute: $[\hat{x}_1 - \hat{x}_2, \hat{p}_1 + \hat{p}_2] = 0$. Such perfect correlations led to the famous EPR paradox on quantum mechanics [22]. The experimental realization of the EPR entangled state and the demonstration of EPR paradox were first done in an optical parametric amplifier [23] in which the two particles are the virtual harmonic oscillators representing two spatially separated modes of optical fields with $\hat{x}_{1,2} \propto \hat{a}^\dagger_{1,2} + \hat{a}_{1,2} \equiv \hat{X}_{1,2}$ and $\hat{p}_{1,2} \propto i(\hat{a}^\dagger_{1,2} - \hat{a}_{1,2}) \equiv \hat{Y}_{1,2}$, where $\hat{a}^\dagger_j$ and $\hat{a}_j$ $(j = 1, 2)$ are the creation and annihilation operators of the two optical fields. Here, $\hat{X}_{1,2}, \hat{Y}_{1,2}$ are related to the amplitude and phase of the corresponding optical fields. Fundamental implication aside, these quantum correlations of orthogonal observables can be employed for the simultaneous measurement of small modulations on the phase and amplitude encoded in one optical field, say, $\hat{X}_1, \hat{Y}_1$ with quantum noise reduced by noise cancelation via $\hat{X}_1 - \hat{X}_2$ and $\hat{Y}_1 + \hat{Y}_2$.

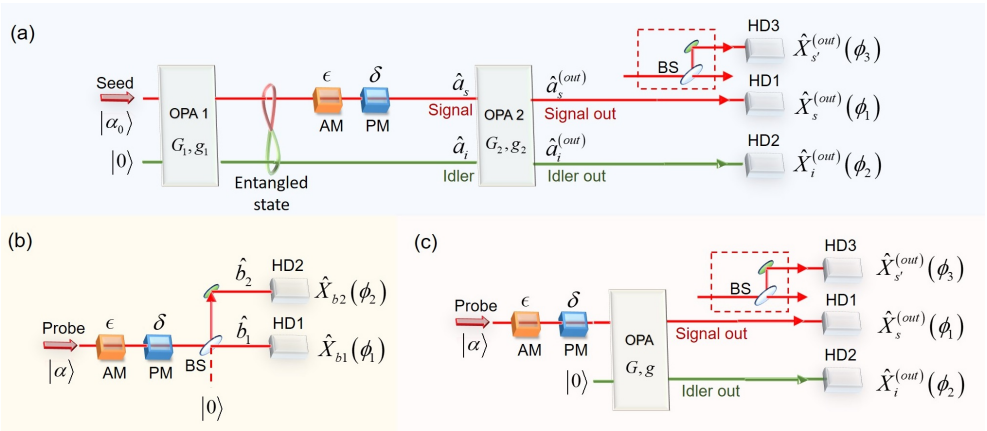

Fig. 1. Schematics for joint measurement of information encoded in multiple non-commuting observables through weak modulations on the probe beam by an amplitude modulator (AM) and a phase modulator (PM). (a) An SU(1,1) interferometer with optical parametric amplifiers (OPA1, OPA2). (b) Classical scheme with a beam splitter (BS). (c) Classical scheme with an optical parametric amplifier (OPA). HD: homodyne detection.

Optics EXPRESS

This idea was first proposed in the form of quantum dense coding [9, 10] and was demonstrated experimentally in the joint measurement of two orthogonal observables with precision beating SNL [11, 12]. We show in the following that such a strategy can be realized with the help of an SU(1,1) interferometer.

Consider the SU(1,1) interferometer depicted in Fig. 1(a), where the beam splitters of a traditional Mach-Zehnder interferometer are replaced by optical parametric amplifiers (OPA) with gain parameters $G_k, g_k (k = 1, 2, G_k^2 - g_k^2 = 1)$. The first optical parametric amplifier (OPA1) creates two fields labeled as signal and idler whose $\hat{X}_{s,i}$ and $\hat{Y}_{s,i}$ have been shown to possess the aforementioned EPR-type correlations $(s, i = 1, 2)$ [23]. The second OPA (OPA2), with the proper phase and gain parameter, is described by [24]

$$\hat{a}_s^{(out)} = G_2\hat{a}_s - g_2\hat{a}_i^\dagger, \hat{a}_i^{(out)} = G_2\hat{a}_i - g_2\hat{a}_s^\dagger, \tag{1}$$

which gives $\hat{X}_s^{(out)} = G_2\hat{X}_s - g_2\hat{X}_i$, $\hat{Y}_i^{(out)} = G_2\hat{Y}_i + g_2\hat{Y}_s$. When $G_2 \gg G_1 > 1$ or $G_2 \approx g_2$, we have $\hat{X}_s^{(out)} \propto \hat{X}_s - \hat{X}_i$, $\hat{Y}_i^{(out)} \propto \hat{Y}_s + \hat{Y}_i$. Hence, the measurement of $\hat{X}_s^{(out)}$ in the signal output and $\hat{Y}_i^{(out)}$ at the idler output of the interferometer by homodyne detection (HD) will be a direct measurement of $\hat{X}_s - \hat{X}_i$ and $\hat{Y}_s + \hat{Y}_i$, which can simultaneously have their fluctuations less than what HUR allows [23]. Note that the technique of using an amplifier to measure $\hat{X}_s - \hat{X}_i$ or $\hat{Y}_s + \hat{Y}_i$ was first introduced by Flurin *et al.* [25] in microwave regime to overcome the thermal noise which would otherwise overwhelm the quantum noise to be measured. We recently generalize this idea to even cover the vacuum quantum noise due to non-ideal detection efficiency [26].

A phase modulation (PM) of $\delta \ll 1$ and an amplitude modulation (AM) $\epsilon \ll 1$ are simultaneously applied to the signal field in $\hat{X}_s$ and $\hat{Y}_s$, respectively, as expressed in terms of a small phase shift $e^{j\delta} \approx 1 + j\delta$ and an amplitude transmission of $e^{-\epsilon} \approx 1 - \epsilon$. The modulated field is then $\hat{a}_s e^{j\delta} e^{-\epsilon} \approx \hat{a}_s(1 + j\delta - \epsilon)$. For an arbitrary modulation signal consists of both phase and amplitude modulation, its modulation signal size is related to δ and ϵ by $\xi(\theta) = \epsilon\cos\theta + \delta\sin\theta$ with $\xi(0) \equiv \epsilon, \xi(\pi/2) \equiv \delta$. The modulation signals δ and ϵ or $\xi(\theta)$ are to be measured. Therefore, through the joint measurement of $\hat{X}_s^{(out)}$ and $\hat{Y}_i^{(out)}$, which can be measured simultaneously with arbitrary precision, the modulation signals encoded in both $\hat{X}_s$ (AM) and $\hat{Y}_s$ (PM) can be simultaneously measured with sensitivity beyond the SNL.

We should mention that we do not make simultaneous measurement on $\hat{X}_s, \hat{Y}_s$, whose precisions are limited by HUR, but rather on $\hat{X}_s - \hat{X}_i$ and $\hat{Y}_s + \hat{Y}_i$, whose precisions are not limited because they commute. On the other hand, experimental limitations such as finite gain will lead to finite non-zero uncertainties for $\hat{X}_s - \hat{X}_i$ and $\hat{Y}_s + \hat{Y}_i$. For an experimental demonstration, we need to define the classical limit of the joint measurement of phase and amplitude for comparison. The classical limit corresponds to the measurement with coherent state probe for the phase and amplitude. Homodyne detection measurement is known to have the quantum-limited sensitivity for phase and amplitude measurement but it can only measure one quadrature-phase amplitude at a time. So, the simplest way to simultaneously obtain information encoded in phase and amplitude of an optical field is to split the field into two with a beam splitter, one for each measurement, as shown in Fig. 1(b). The measurement sensitivity of this scheme is limited by the shot noise from the coherent state and will correspond to the shot noise limit (SNL) that we try to beat in our experiment.

However, the SU(1,1) interferometer (SUI) shown in Fig. 1(a) operates under completely different mechanism from the traditional interferometric methods such as homodyne detection. It uses OPA2 to enhance the signal while employs the correlated fields from OPA1 to reduce the noise amplified by OPA2 via destructive quantum interference [27–29]. It exhibits different noise level from the BS scheme in Fig. 1(b). So, for a fair comparison with SUI, we consider the amplifier scheme in Fig. 1(c), where, similar to the BS scheme, a parametric amplifier is used to split the input field into two for simultaneous measurement. The other input to the amplifier is in

Optics EXPRESS

vacuum similar to the BS scheme in Fig. 1(b).

To compare all three schemes in Fig. 1 with equal footings, we resort to signal-to-noise ratio (SNR), which depends on the power levels of both the detected signal and noise. For a probe with weak modulated phase signal δ and amplitude signal ϵ, our theoretical analysis [24] shows that the SNRs for the BS scheme in Fig. 1(b) and the amplifier scheme in Fig. 1(c) are given by

$$SNR_{BS}(\hat{X}_{b_1}) = 2I_{ps}\epsilon^2, \quad SNR_{BS}(\hat{Y}_{b_2}) = 2I_{ps}\delta^2; \tag{2}$$

$$SNR_{Amp}(\hat{X}_s^{(out)}) = \frac{4G^2 I_{ps}\epsilon^2}{G^2+g^2}, \quad SNR_{Amp}(\hat{Y}_i^{(out)}) = \frac{4g^2 I_{ps}\delta^2}{G^2+g^2}, \tag{3}$$

where subscript b_1, b_2 denotes the outputs of the BS and s, i denote the signal and idler output fields of the parametric amplifier with the gain parameters G, g satisfying $G^2 - g^2 = 1$. $I_{ps} = |\alpha|^2$ is the photon number or intensity of the probe sensing field. It is clear from Eqs. (2) and (3) that the amplifier scheme at large gain $g \gg 1$ gives the same SNRs as the BS scheme for the joint measurement of the phase and amplitude modulations δ, ϵ. This SNR will correspond to the SNL of the sensitivity in the joint phase and amplitude measurement.

For the SUI shown in Fig. 1(a), the maximum sensitivity occurs at the dark fringe when the outputs intensity are at the minimum.Under this condition, destructive quantum interference leads to quantum noise cancelation and minimum noise for all quadrature-phase amplitudes at the two outputs [24, 27–29]. In the meantime, the signals of non-commuting observable encoded on probe beam are amplified by OPA2 for SNR improvement. With $G_2 \gg G_1 > 1$, it can be shown [24] that the SNRs for the SUI scheme are

$$SNR_{SUI}(\hat{X}_s^{(out)}) = 2(G_1+g_1)^2 I_{ps}\epsilon^2, \tag{4}$$

$$SNR_{SUI}(\hat{Y}_i^{(out)}) = 2(G_1+g_1)^2 I_{ps}\delta^2, \tag{5}$$

where $I_{ps} = G_1^2|\alpha_0|^2$ is the intensity of the probe sensing field right before the devices introducing modulation signals. It is clear that the SUI scheme has the SNRs improved by a factor of $(G_1+g_1)^2$ as compared to the classical schemes under the condition of equal I_{ps}. This improvement in phase measurement was demonstrated in SUI before [18–20]. Here, we show that the sensitivity in amplitude measurement can be improved as well, simultaneously with the phase measurement. It can be shown [24] that Eqs. (4) and (5) also stands for an arbitrary modulation signal $\xi(\theta) = \epsilon\cos\theta + \delta\sin\theta$ but we need to measure $\hat{X}^{(out)}(\theta) = \hat{a}e^{-i\theta} + \hat{a}^\dagger e^{i\theta}$. Moreover, since SU(1,1) interferometers are not sensitive to detection losses [16–18, 20, 21, 24, 30], we can further split the output beams with negligible degradation of the SNRs and achieve joint measurement on multiple modulation signals at arbitrary quadrature angles [24].

3. Experiment setup

We next implement experimentally the three schemes in Fig. 1. The signals of weakly modulated amplitude (ϵ) and phase (δ) are encoded on $\hat{X}_s = \hat{X}_s(0)$ and $\hat{Y}_s = \hat{X}_s(\pi/2)$ ($\hat{X}_s(\phi) \equiv \hat{a}_s^\dagger e^{i\phi} + \hat{a}_s e^{-i\phi}$) of the probe beam by applying sinusoidal modulation signal at 0.8 and 1.2 MHz on the amplitude modulator (AM) and phase modulator (PM), respectively. This probe is a classical coherent beam for the classical schemes in Figs. 1(b) and 1(c), while the probe for the SUI scheme in Fig. 1(a) is a quantum correlated beam from OPA1. In all cases, the probe beam intensity I_{ps} is adjusted to be the same for fair comparison, and the amplifier gains for OPA in Fig. 1(c) and for OPA2 in Fig. 1(a) are also the same to ensure equal signal gain. The operation of the classical amplifier scheme in Fig. 1(c) is straightforward. For the best sensitivity, the SUI is operated at dark fringe where the output intensity at both signal and idler ports are at minimum [16, 18, 24].

The details of the experimental setup for the scheme of SU(1,1) interferometer is shown in Fig. 2. There are two fiber-based OPAs in the scheme. Each OPA consists of 300 m long dispersion

Optics EXPRESS

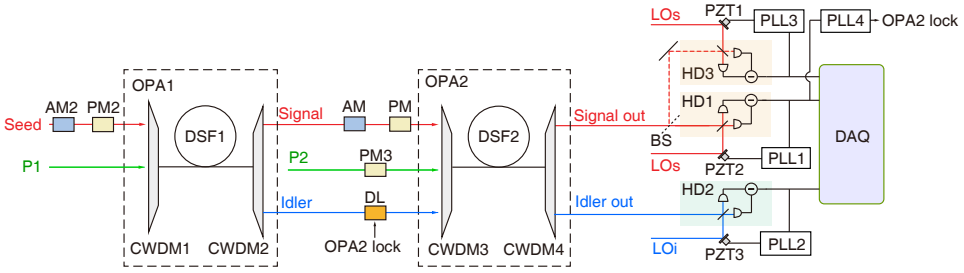

Fig. 2. **Experimental setup.** The SU(1,1) interferometer (SUI) is formed with OPA1 and OPA2 with seed injection at OPA1. AM, amplitude modulator; PM, phase modulator; P1, P2, pulsed pumps; DSF, dispersion shifted fiber; CWDM, coarse wavelength division multiplexer; BS, 50/50 beam splitter; DL, delay line; OPA2 lock, locking signal for OPA2; PLL, phase locking loops; LOs, LOi, local oscillators; PZT, Piezo-Electric ceramic Transducer; HD, homodyne detection; DAQ, data acquisition system.

shifted fiber (DSF) and two coarse wavelength division multiplexers (CWDM) for separation and combination of fields at different wavelength [31]. The zero-dispersion wavelength of DSF is 1552.5nm. In order to efficiently enhance the gain of OPA under a moderate average pump power, each DSF is pumped with a mode locked pulse train, whose repetition rate and pulse width are about 36.9 MHz and 5 ps, respectively. The pulsed pump with full width at half maximum (FWHM) of 0.7 nm is centered at 1552.6 nm to ensure the phase matching of FWM is satisfied. OPA1 generates the entangled signal and idler beams at 1550 nm band [31]. At the output of DSF1, the seed injection of input signal pulses centering at 1570.8 nm is amplified. The amplification of the signal beam is accompanied by a idler beam with wavelength around 1535 nm. The two fiber-based OPAs are identical, except for their inputs and pump powers. OPA2 is a phase sensitive amplifier, because it has both the signal and the idler inputs with non-zero intensity from OPA1. The signal beam out of OPA1 successively propagates through an amplitude modulator (AM) and a phase modulator (PM) so as to encode information onto the two or more quadrature-phase amplitudes. The encoded signal beam is then amplified by OPA2 and comes out at both the signal and idler output ports of the SUI. When two encoded modulations $\xi(\theta_1)$, $\xi(\theta_2)$ $(\theta_1 \neq \theta_2)$ are measured, the signal and idler outputs of SU(1,1) interferometer are detected with homodyne detection systems HD1 and HD2, respectively, at the matching local oscillator phases, respectively. When three encoded modulations $\xi(\theta_1)$, $\xi(\theta_2)$, $\xi(\theta_3)$ $(\theta_1 \neq \theta_2 \neq \theta_3)$ are measured, the signal output of SUI is further split by inserting a 50/50 BS, whose outputs are measured by HD1 and HD3, respectively. During the measurement, the phase of local oscillator for each set of HD is properly set. The measurement results are obtained by analyzing the photo-currents of all the HDs with a data acquisition system (DAQ). In the DAQ system, the photo-currents of all HDs are converted to digital signal traces at sampling rate of 5.71MSample/s and sample length of 16380 samples per trace. Each trace is analyzed by fast Fourier transformation (FFT) for power spectrum analysis. The spectrum is averaged over 500 traces to reduce measurement fluctuation. The power on the spectrum is normalized to the shot noise level at the same power of local oscillator.

In the experiment, the preparation of the optical light sources, including the pumps of OPAs (P1, P2), the injected seed signal, and the local oscillator (LO) of each homodyne detection (HD) device, and the realization of mode-matching between the two OPAs for best performance of the interferometer are described in a previous publication [29].

The improvement in SNR of joint measurement occurs under the two conditions: (i) the phase between pump and two inputs of OPA2, $\varphi = 2\varphi_{p_2} - \varphi_s - \varphi_i$, is locked to ensure OPA2

Optics EXPRESS

is operating in the deamplification condition, where φ_{p_2} is the phase of pump P2, φ_s and φ_i are the phase of signal and idler input; and (ii) the phase ϕ of the local oscillator for each HD device is properly locked. To achieve this, we pass the injected seed sequentially through an amplitude modulator (AM2) and a phase modulator (PM2) in order to generate phase locking signals. AM2 is modulated at the frequencies of 0.3125 and 1.875 MHz. PM2 is modulated at the frequencies of 0.625 and 1.875 MHz. In this case, both the modulated signals of AM2 and PM2 are transferred to the amplified signal and idler beams of OPA1 and OPA2. The relative phase ϕ is locked by feeding the ac output of the corresponding HD to the digital phase locking loop PLL1/PLL2/PLL3, and by loading the feedback signal of PLL1/PLL2/PLL3 to the piezo-electric transducer PZT1/PZT2/PZT3 [31]. To measure the encoded amplitude signal ϵ, we perform measurement of $\hat{X}_s^{(out)}(0)$ with HD1by exploiting the sinusoidal modulation signal of PM2 at 0.625 MHz to lock the relative phase of HD1 to $\phi_1 = 0$. In the meanwhile, we can lock the relative phase of HD2 to $\phi_2 = \pi/2$ by exploiting the sinusoidal modulation signal of AM2 at 0.3125 MHz to measure $\hat{X}_i^{(out)}(\pi/2)$ for the encoded phase signal δ, and lock the relative phase of HD3 to $\phi_3 = \pi/4$ by using the combined sinusoidal modulation signals of AM2 and PM2 at 1.875 MHz, in order to obtain the encoded quadrature amplitude signal $\xi(\pi/4)$. The relative phase φ which determines the operation condition of OPA2 is locked by passing P2 through PM3 with the sinusoidal modulation signal at 1.5625 MHz. Since the modulated signal of PM3 is transferred to the signal and idler outputs of OPA2, the deamplication condition of OPA2 $\varphi = \pi$ can be achieved by feeding the ac output of the HD1 at 1.5625 MHz to PLL4 and loading the feedback signal of PLL4 to the delay line (DL) on the idler input of OPA2.

4. Results

Simultaneous measurements of the modulation signals ϵ and δ are performed for the schemes with amplifiers (Fig. 1(a) and (c)) by homodyne measurement at signal and idler output ports with detection efficiencies of 67% and 58%, respectively. The relative phase ϕ_1 (ϕ_2) between LOs (LOi) and the signal (idler) output beam in HD1 (HD2) is locked to $\phi_1 = 0$ ($\phi_2 = \pi/2$). Figures 3(a) and 3(b) respectively present the joint measurement results obtained by HD1 and HD2. During this measurement, the intensity of probe I_{ps} is about 2 nW. The power gains (equivalent to G_1^2 and G_2^2) for OPA1 and OPA2 are 2 and 9. The blue traces in Fig. 3 are achieved by SUI (Fig. 1(a)) with a seed injection of 1 nW (input of OPA1), while the red traces are acquired with classical scheme (Fig. 1(c)) by setting P1 to zero and increasing the seed injection to 2 nW to keep the same I_{ps}. The peaks at 0.8 and 1.2 MHz in Figs. 3(a) and 3(b) correspond to the power of modulation signals ϵ and δ, respectively. It can be seen that the signal powers for blue and red traces are about the same but the noise floor of the blue trace is lower than that of the red trace by about 20% and 22%, respectively, due to destructive quantum interference between the signal and the idler fields out of OPA1 [29]. For the phase and amplitude modulation signals ϵ and δ, the SNRs read from the blue traces are 1.62±0.04 and 1.55±0.04, respectively, which are better than the SNRs of 1.29±0.03 and 1.22±0.03 extracted from the red traces. We note that the value of measured noise power for signal and idler fields cannot be directly deduced from the simple single mode theory (see Sec. 2 and Ref. [24]) due to the multimode nature of our pulse pumped fiber optical parametric amplifiers [32].

For the completeness of comparison, we also implement the BS scheme in Fig. 1(b), which is achieved by blocking the two pumps P1 and P2 so that OPA1 and OPA2 simply function as transmission media. After splitting the probe beam with a 50/50 BS, we perform joint measurement of ϵ by HD1 and δ by HD2 at each output port of BS (b1 and b2). The results are shown as the black traces in Figs. 3(c) and 3(d), respectively. The extracted SNRs of ϵ and δ are 1.03±0.03 and 1.01±0.03 after correcting the transmission efficiency of OPA2. Ideally from Eqs. (2) and (3), the SNRs by the classical methods in Figs. 1(b) and 1(c) should be the same at large amplifier gain. However, Fig. 3 clearly shows a difference. This is because the output

Optics EXPRESS

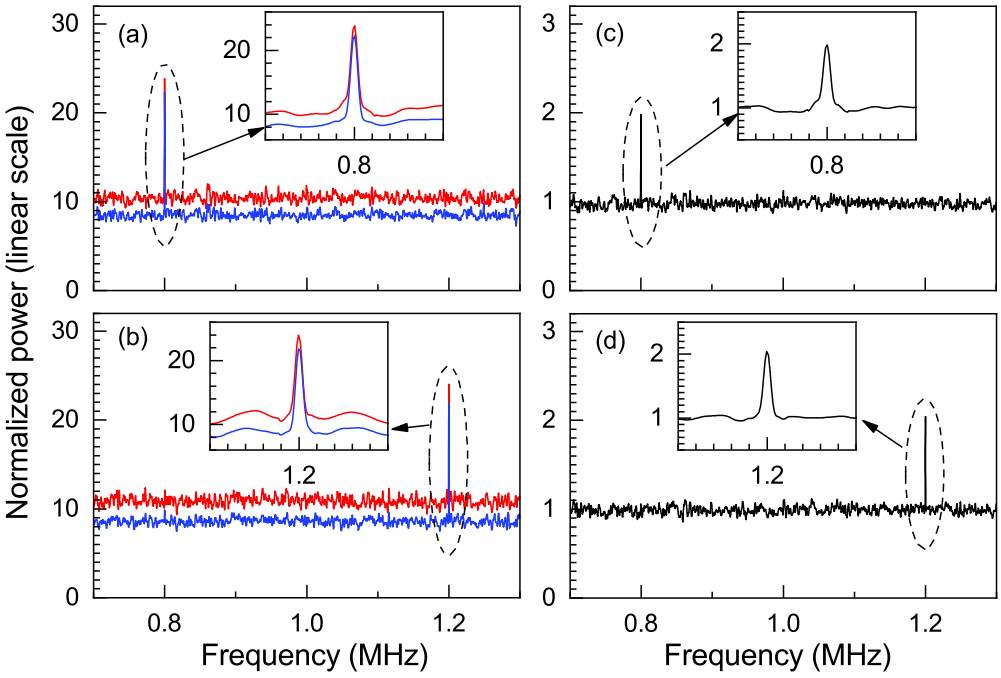

Fig. 3. Joint measurement of the amplitude and phase modulations ϵ and δ under different situations. (a) and (b) are the results of simultaneous measurement by HD1 and HD2 on $\hat{X}_s^{(out)}, \hat{Y}_i^{(out)}$, respectively, for the SUI scheme in Fig. 1(a) (red traces) and classical amplifier scheme 1(c) (blue traces). (c) and (d) are results from the beam splitter scheme in Fig. 1(b). The peaks at 0.8 MHz and 1.2 MHz correspond to the power of AM and PM modulation signals ϵ and δ, respectively. The measurement results are normalized to the shot noise level at same local oscillator power.

noise of the conventional OPA is higher than the shot noise, so the SNR for amplifier scheme is less sensitive to the loss at detection than the direct homodyne measurement for the BS scheme. Therefore, the amplifier scheme in Fig. 1(c) is more suitable as a classical measurement scheme for the comparison with the quantum scheme of SU(1,1) interferometer in Fig. 1(a).

Although our results are valid for all frequency components because the homodyne detections at two outputs are independent, for the clarity of demonstration, we choose different frequencies for the phase and amplitude modulations in the experiment above. This corresponds to the case when the two modulations are uncorrelated. If the two modulations are at the same frequency and they are correlated, it will result in a modulation at a different quadrature-phase amplitude $\xi(\theta) = \epsilon \cos\theta + \delta \sin\theta$.

Fortunately, the SUI in Fig. 1(a) can be arranged for the measurement of $\xi(\theta)$ by performing homodyne detection with LO phase set at $\phi_{LO} = \theta$. With a change in homodyne detection angle, one would expect a different, likely higher, noise level. However, this is not true for SUI because its working principle is quantum destructive interference for noise cancelation and the noise is the lowest at dark fringe for all quadrature-phase amplitudes. The measured SNR for the modulation signal $\xi(\theta)$ with an arbitrary angle θ is the same as that in Eqs. (4) and (5) [24]. So, we can simultaneously measure $\xi(\theta)$ at one outport and $\xi(0) = \epsilon$ at the other with improved SNR for both. Figure 4 shows the results with all experimental conditions the same as Fig. 3 except that a modulation signal at 1.0 MHz is applied to both AM and PM equally for $\xi(\pi/4)$ and the phase of HD2 is set at $\phi_2 = \pi/4$. The blue trace is again for SUI and red one for the amplifier scheme. We

Optics EXPRESS

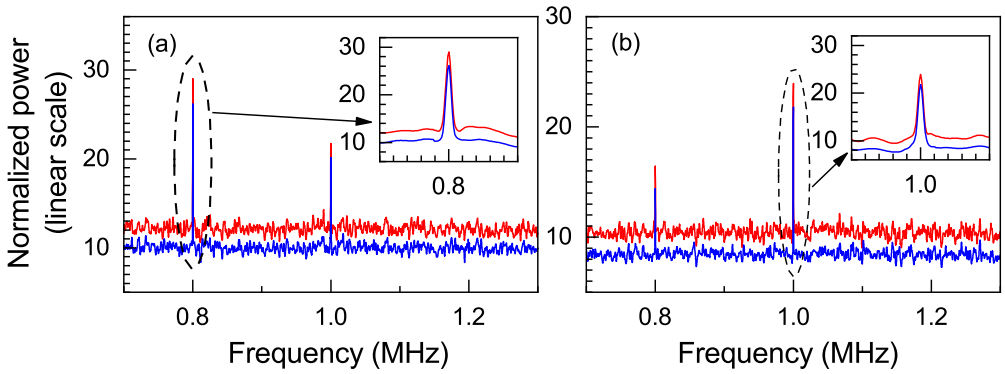

Fig. 4. Information of ϵ (at 0.8MHz) and $\xi(\pi/4)$ (at 1.0MHz) encoded in non-orthogonal quadrature-phase amplitudes $\hat{X}_s(0)$ and $\hat{X}_s(\pi/4)$ simultaneously measured by (a)HD1 and (b)HD2, respectively. Blue and red traces represent the results of SUI (Fig. 1(a)) and conventional OPA (Fig. 1(c)), respectively.

find the SNRs of $\xi(0) = \epsilon$ and $\xi(\pi/4)$ extracted from blue traces (1.61±0.04 and 1.57±0.04) are better than those from red traces (1.3±0.03 and 1.27±0.03), leading to improved simultaneous measurement of information encoded in non-commuting observables of $\hat{X}_s(0)$ and $\hat{X}_s(\pi/4)$ of the probe. Notice that because $\xi(0) = \epsilon$ and $\xi(\pi/4)$ are non-orthogonal, their respective projections appear in the measurement corresponding to other quantities.

Furthermore, because of the detection loss tolerant property [24], the SUI can be used to perform quantum enhanced joint measurement of information encoded in more than two quadrature-phase amplitudes. This is achieved by splitting the outputs of interferometer further into more beams for multiple simultaneous measurement, as shown in the dashed boxes in Fig. 1(a) and (c). Since the noise levels out of the amplifiers are much higher than the vacuum noise level, splitting each output into two will not distinctly reduce the SNR [24]. This is different from the BS scheme in Fig. 1(b). In the experiment, in addition to the weak modulation signals at 0.8 MHz and 1.2 MHz on AM and PM that encode information on the two orthogonal observables $\hat{X}_s$ and $\hat{Y}_s$, the modulation signal at 1.0 MHz is simultaneously loaded on both AM and PM so that the information of $\xi(\pi/4)$ is encoded on the probe sensing beam as well. $\xi(\pi/4)$ is measured by a third homodyne detection device (HD3) with detection efficiency of about 80% in the signal output port after splitting the signal output into two with a 50/50 BS (dashed boxes in Fig. 1(a) and 1(c)). The results in Figs. 5(a), 5(b) and 5(c) are obtained by HD1, HD2, and HD3 with their relative phases locked at $\phi_1 = 0$, $\phi_2 = \pi/2$, and $\phi_3 = \pi/4$, respectively. The experimental conditions are the same as those in Fig. 3. Again, the blue traces are for the SUI and the red ones are for the classical amplifier scheme in Fig. 1(c). Similar to Fig. 4, projections of non-orthogonal quantities appear in all the figures. In each plot of Fig. 5, the signal powers of ϵ, δ and $\xi(\pi/4)$ extracted from the blue and red traces, including the signals of full size or projected size, are about the same, but the noise floor of blue traces is 20% lower than that of the red ones. The best SNRs of modulation signal ϵ, δ and $\xi(\pi/4)$ extracted from the blue traces are 1.6±0.04, 1.56±0.04, and 1.61±0.04, respectively, while those from the red traces are 1.25±0.03, 1.21±0.03, 1.27±0.03, respectively. Therefore, we achieve joint measurement of information in three non-commuting quadrature-phase amplitudes with sensitivity beyond the SNL. Notice that, even if the total detection efficiencies for ϵ and $\xi(\pi/4)$ are about 50% lower than that for δ, the SNR improvement for ϵ, $\xi(\pi/4)$ and δ is all about the same in Fig. 5. Thus, we demonstrate that the SNR is tolerant to the detection losses. It is worth noting that the feature of detection loss tolerance depends on the gain of OPA2 [28]. The higher the gain of OPA2 is, the better the loss

Optics EXPRESS

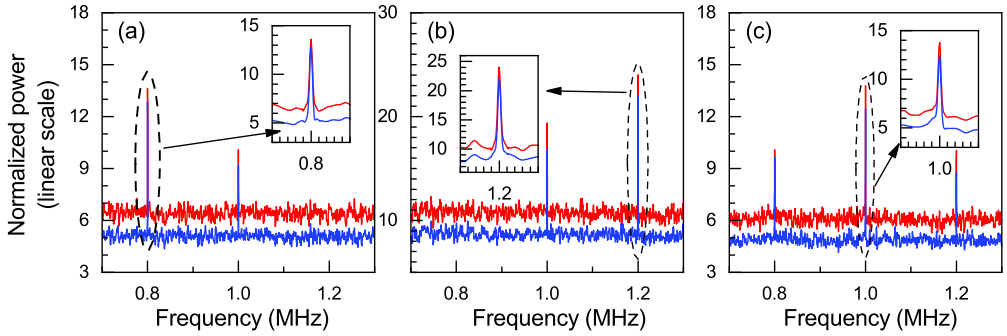

Fig. 5. Information of modulations ϵ (at 0.8MHz), δ (at 1.2MHz) and $\xi(\pi/4)$ (at 1.0MHz) encoded in three non-commuting quadrature-phase amplitudes of $\hat{X}_s, \hat{Y}_s, \hat{X}_s(\pi/4)$ jointly measured by (a)HD1, (b)HD2, and (c)HD3, respectively. Blue and red traces represent the results of SUI (Fig. 1(a)) and conventional OPA (Fig. 1(c)), respectively.

tolerance performance of SUI is. Under the current experimental conditions, further splitting the signal output for measuring the observables with total number greater than 3 will result in reduced SNR. But we can simultaneously measure 4 observables with SNR beyond SNL if the idler output beam is split into two as well. Instead, we can resort to an indirect method to extract the information encoded in arbitrary number of quadrature-phase amplitudes by post-processing the photo-currents of two HDs with their LO phase difference of $\pi/2$ [24]. We will discuss its experimental implementation elsewhere [33].

5. Conclusion and discussions

Using an SU(1,1) interferometer, we demonstrate that the sensitivity can beat the classical shot noise limit in the joint measurement of information encoded in multiple non-commuting observables, including the phase and amplitude as well as an arbitrarily rotated quadrature-phase amplitude. Theoretically, the improvement over the classical schemes is unlimited in principle.

Although the measured SNR is not sensitive to the transmission and detection losses at the output ports of OPA2, it decreases with the increase of losses before the inputs of OPA2. In our experiment, we only observed the improvement of about 20% in SNR when comparing with the classical scheme. This is mainly due to the transmission loss (45% for signal beam and 40% for idler beam) introduced in coupling light out of the OPA1 into the OPA2 and the temporal mode mismatch between OPA1 and OPA2 [31, 32]. The former can be overcome by improving the transmission efficiency of the optical components placed between the two amplifiers, while the latter can be surmounted by properly managing the dispersion of the nonlinear media of the two OPAs. If the transmission loss is 0 for ideal case, the SNR improvement over classical limit is expected to be 35%.

The gain achievable in our system is also a limitation factor for better performance. The main reason for choosing the power gain of 9 for OPA2 is the self-phase modulation (SPM) effect of pump pulse. When the pump power gets higher, the SPM effect becomes stronger and introduces more mode mismatch between OPA1 and OPA2 [32]. On the other hand, our theoretical analysis shows that when the power gain of OPA2 is higher than that of OPA1 by about 4 times, the SNR will start to saturate the maximum SNR obtainable for OPA2 with infinite gain [24]. Thus, as a trade-off between the better SNR improvement and tolerable SPM effect in OPA2, the power gain of OPA2 is adjusted to be 9 when the power gain of OPA1 is 2.

Compared to the joint measurement schemes in Ref. [11, 12], our scheme, which utilizes the merits of the SU(1,1) interferometer, leads to the joint measurement of information in more than

Optics EXPRESS

two arbitrary non-commuting quadrature-phase amplitudes. Particularly, it should be emphasized that our scheme can overcome the extra noise (quantum and classical) encountered during the detection process [24], and has practical implication and significance in quantum metrology.

Ever since the first experimental implementation of the SU(1,1) interferometer with light fields [15, 18], it has been realized with atoms in Bose-Einstein condensate [34], phonons in opto-mechanical systems [35], microwaves in low noise RF amplifiers [25], and a combined atom-photon system in hybrid atom-light interferometers [36]. The wide applications of SUI is a result of its ability to mix different types of waves. Thus, our scheme of utilizing SUI for the joint multi-parameter measurement has broader significance in precision measurement of a variety of physical observables.

Funding

National Key Research and Development Program of China (2016YFA0301403); Program 973 of China (2014CB340103); National Natural Science Foundation of China (91736105, 11527808); Project 111 (B07014).

References

1. C. M. Caves, "Quantum-mechanical noise in an interferometer," Phys. Rev. D **23**, 1693–1708 (1981).
2. M. Xiao, L.-A. Wu, and H. J. Kimble, "Precision measurement beyond the shot-noise limit," Phys. Rev. Lett. **59**, 278–281 (1987).
3. P. Grangier, R. E. Slusher, B. Yurke, and A. LaPorta, "Squeezed-light–enhanced polarization interferometer," Phys. Rev. Lett. **59**, 2153–2156 (1987).
4. P. C. Humphreys, M. Barbieri, A. Datta, and I. A. Walmsley, "Quantum enhanced multiple phase estimation," Phys. Rev. Lett. **111**, 070403 (2013).
5. M. G. Genoni, M. G. A. Paris, G. Adesso, H. Nha, P. L. Knight, and M. S. Kim, "Optimal estimation of joint parameters in phase space," Phys. Rev. A **87**, 012107 (2013).
6. P. J. D. Crowley, A. Datta, M. Barbieri, and I. A. Walmsley, "Tradeoff in simultaneous quantum-limited phase and loss estimation in interferometry," Phys. Rev. A **89**, 023845 (2014).
7. T. Baumgratz and A. Datta, "Quantum enhanced estimation of a multidimensional field," Phys. Rev. Lett. **116**, 030801 (2016).
8. M. Szczykulska, T. Baumgratz, and A. Datta, "Multi-parameter quantum metrology," Adv. Physics: X **1**, 621–639 (2016).
9. S. L. Braunstein and H. J. Kimble, "Dense coding for continuous variables," Phys. Rev. A **61**, 042302 (2000).
10. J. Zhang and K. Peng, "Quantum teleportation and dense coding by means of bright amplitude-squeezed light and direct measurement of a bell state," Phys. Rev. A **62**, 064302 (2000).
11. X. Li, Q. Pan, J. Jing, J. Zhang, C. Xie, and K. Peng, "Quantum dense coding exploiting a bright einstein-podolsky-rosen beam," Phys. Rev. Lett. **88**, 047904 (2002).
12. S. Steinlechner, J. Bauchrowitz, M. Meinders, H. Müller-Ebhardt, K. Danzmann, and R. Schnabel, "Quantum-dense metrology," Nat. Photonics **7**, 626–630 (2013).
13. B. Yurke, S. L. McCall, and J. R. Klauder, "Su(2) and su(1,1) interferometers," Phys. Rev. A **33**, 4033–4054 (1986).
14. W. N. Plick, J. P. Dowling, and G. S. Agarwal, "Coherent-light-boosted, sub-shot noise, quantum interferometry," New J. Phys. **12**, 083014 (2010).
15. J. Jing, C. Liu, Z. Zhou, Z. Y. Ou, and W. Zhang, "Realization of a nonlinear interferometer with parametric amplifiers," Appl. Phys. Lett. **99**, 011110 (2011).
16. Z. Y. Ou, "Enhancement of the phase-measurement sensitivity beyond the standard quantum limit by a nonlinear interferometer," Phys. Rev. A **85**, 023815 (2012).
17. A. M. Marino, N. V. Corzo Trejo, and P. D. Lett, "Effect of losses on the performance of an su(1,1) interferometer," Phys. Rev. A **86**, 023844 (2012).
18. F. Hudelist, J. Kong, C. Liu, J. Jing, Z. Y. Ou, and W. Zhang, "Quantum metrology with parametric amplifier-based photon correlation interferometers," Nat. Commun. **5**, 3049 (2014).
19. B. E. Anderson, P. Gupta, B. L. Schmittberger, T. Horrom, C. Hermann-Avigliano, K. M. Jones, and P. D. Lett, "Phase sensing beyond the standard quantum limit with a variation on the su(1,1) interferometer," Optica **4**, 752–756 (2017).
20. M. Manceau, G. Leuchs, F. Khalili, and M. Chekhova, "Detection loss tolerant supersensitive phase measurement with an su(1,1) interferometer," Phys. Rev. Lett. **119**, 223604 (2017).
21. M. Manceau, F. Khalili, and M. Chekhova, "Improving the phase super-sensitivity of squeezing-assisted interferometers by squeeze factor unbalancing," New J. Phys. **19**, 013014 (2017).
22. A. Einstein, B. Podolsky, and N. Rosen, "Can quantum-mechanical description of physical reality be considered complete?" Phys. Rev. **47**, 777–780 (1935).

Optics EXPRESS

23. Z. Y. Ou, S. F. Pereira, H. J. Kimble, and K. C. Peng, "Realization of the einstein-podolsky-rosen paradox for continuous variables," Phys. Rev. Lett. **68**, 3663–3666 (1992).
24. J. Li, Y. Liu, L. Cui, N. Huo, S. M. Assad, X. Li, and Z. Y. Ou, "Joint measurement of multiple noncommuting parameters," Phys. Rev. A **97**, 052127 (2018).
25. E. Flurin, N. Roch, F. Mallet, M. H. Devoret, and B. Huard, "Generating entangled microwave radiation over two transmission lines," Phys. Rev. Lett. **109**, 183901 (2012).
26. J. Li, Y. Liu, N. Huo, L. Cui, X. Li, and Z. Y. Ou, "Loss-tolerant measurement of continuous-variable quantum entanglement with the aid of a high gain parametric amplifier," arXiv preprint arXiv:1808.10258 (2018).
27. Z. Y. Ou, "Quantum amplification with correlated quantum fields," Phys. Rev. A **48**, R1761–R1764 (1993).
28. J. Kong, F. Hudelist, Z. Y. Ou, and W. Zhang, "Cancellation of internal quantum noise of an amplifier by quantum correlation," Phys. Rev. Lett. **111**, 033608 (2013).
29. X. Guo, X. Li, N. Liu, and Z. Y. Ou, "Quantum information tapping using a fiber optical parametric amplifier with noise figure improved by correlated inputs," Sci. Reports **6**, 30214 (2016).
30. C. Sparaciari, S. Olivares, and M. G. A. Paris, "Gaussian-state interferometry with passive and active elements," Phys. Rev. A **93**, 023810 (2016).
31. X. Guo, N. Liu, Y. Liu, X. Li, and Z. Y. Ou, "Generation of continuous variable quantum entanglement using a fiber optical parametric amplifier," Opt. Lett. **41**, 653 (2016).
32. X. Guo, N. Liu, X. Li, and Z. Y. Ou, "Complete temporal mode analysis in pulse-pumped fiber-optical parametric amplifier for continuous variable entanglement generation," Opt. Express **23**, 29369 (2015).
33. Y. Liu, J. Li, L. Cui, N. Huo, S. M. Assad, X. Li, and Z. Ou, In preparation for publication, see fig. 5 at preprint arXiv:1712.01553v2 (2017).
34. D. Linnemann, H. Strobel, W. Muessel, J. Schulz, R. Lewis-Swan, K. V. Kheruntsyan, and M. K. Oberthaler, "Quantum-enhanced sensing based on time reversal of nonlinear dynamics," Phys. Rev. Lett. **117**, 013001 (2016).
35. H. F. Cheung, Y. S. Patil, L. Chang, S. Chakram, and M. Vengalattore, "Nonlinear phonon interferometry at the heisenberg limit," arXiv preprint arXiv:1601.02324 (2016).
36. B. Chen, C. Qiu, S. Chen, J. Guo, L. Chen, Z. Y. Ou, and W. Zhang, "Atom-light hybrid interferometer," Phys. Rev. Lett. **115**, 043602 (2015).